

# Cone beam computed tomography evaluation of sphenoid sinus in different sagittal skeletal pattern

## Purpose

The purpose of this study is to explore sphenoid sinus variations in individuals with various sagittal skeletal anomalies using cone-beam computed tomography (CBCT).

## Materials and Methods

We retrospectively analyzed sphenoid sinus pneumatization on CBCT images of 126 patients aged 18–86 years. The anteroposterior skeletal relationships of the maxilla and mandible were classified as skeletal class I, II or III using the A point–nasion–B point (ANB) angle measured in the sagittal plane. The extensions of the sphenoid sinus were evaluated on three planes including axial, sagittal and coronal sections.

## Results

The study population consisted of 84 females (66.7%) and 42 males (33.3%), including 52 (41.3%) class I, 38 (30.1%) class II, and 36 (28.6%) class III cases. The conchal type of sphenoid sinus was not encountered. Presellar sinuses were detected in only 3 (5.8%) class I cases. Incomplete sinuses were detected in 16 (30.8%) class I, 7 (18.4%) class II, and 15 (41.7%) class III cases. Complete sinuses were detected in 33 (63.4%) class I, 31 (81.6%) class II, and 21 (58.3%) class III cases. Lateral extensions were found in 103 (40.9%) of the 252 sinus walls: 33 (31.7%) in class I, 45 (59.2%) in class II, and 25 (34.7%) in class III sinuses.

## Conclusion

Regional sphenoid sinus anatomy can be carefully examined via CBCT. The sphenoid sinus pneumatization did not differ significantly in patients exhibiting different types of sagittal skeletal closure, with the exception of the lesser wing type.

**Keywords:** Sphenoid sinus, cone beam computed tomography, anatomy, anomalies, malocclusions

## Introduction

The sphenoid sinus is the most inaccessible and variable paranasal sinus and is in the middle of the cranial base. Several important anatomical structures include the optic nerve in the superolateral region, the internal carotid artery in the lateral wall, and the vidian nerve at the base surround the sinus (1). Pneumatization of the sinus enlarges the natural space accessible to large cranial base areas. Pneumatization commences in the ostia at 6 months, and the posterior, inferior, and lateral progress, and the sinus reaches its final size after 14 years (2, 3). The cavernous sinuses surrounding sphenoid sinus laterally, ethmoid air cells anteriorly, the choana inferiorly, the clivus posteriorly, planum sphenoidale, and the pituitary fossa superiorly. The sinus might exhibit various extents of pneumatization, and the size, shape, and pneumatization type vary individually; as has been well documented (4, 5–7). Sometimes, pneumatization extends into the vomer, occipital, ethmoid, and palatine bones; the anterior and

Selin Yesiltepe<sup>1</sup> ,  
Elif Kurtuldu<sup>2</sup> ,  
Ibrahim Sevki Bayrakdar<sup>3</sup> ,  
Ahmet Berhan Yilmaz<sup>4</sup> 

ORCID IDs of the authors: S.Y. 0000-0002-6857-1411;  
E.K. 0000-0003-4844-4906; I.Ş.B. 0000-0001-5036-9867;  
A.B.Y. 0000-0001-5494-0290

<sup>1</sup>Department of Oral and Maxillofacial Radiology, Faculty of Dentistry, Adnan Menderes University, Aydın, Türkiye

<sup>2</sup>Dentomaxillofacial Specialist, Sakarya Oral and Dental Health Center, Ministry of Health, Sakarya, Türkiye

<sup>3</sup>Department of Oral and Maxillofacial Radiology, Faculty of Dentistry, Eskişehir Osmangazi University, Eskişehir, Türkiye

<sup>4</sup>Department of Oral and Maxillofacial Radiology, Faculty of Dentistry, Ataturk University, Erzurum, Türkiye

Corresponding Author: Selin Yeşiltepe

E-mail: dt\_selin@yahoo.com

Received: 24 September 2021

Revised: 12 January 2022

Accepted: 20 February 2022

DOI: 10.26650/eor.20221000193

posterior clinoid processes; the lesser and greater wings; the clivus; and the pterygoid process and plates (2, 8). Bone which covers the vidian, and maxillary nerves and the carotid arteries may be thin or even absent. In these cases, these structures are under iatrogenic damage depending on the pneumatization extent (9).

The extent and direction of sphenoid sinus pneumatization is important when planning surgery. The sinus anatomy and its variations must be well understood. As far as we know, no study has yet explored sphenoid sinus variations in individuals with various sagittal skeletal anomalies. Here, we used cone-beam computed tomography (CBCT) to explore this topic in individuals of skeletal classes I, II, and III. The null hypothesis tested in the present study is that the frequencies of sphenoid sinus variations do not differ among individuals having different sagittal skeletal patterns.

## Material and Methods

### Ethical statement

The Clinical Research Ethical Committee of Atatürk University approved the research protocol on 03/01/2019, with protocol number 2019/21 and the work adhered to all relevant principles of the Declaration of Helsinki and amendments and revisions thereof.

### Study population

We retrospectively analyzed sphenoid sinus pneumatization on CBCT images of 126 patients aged 18–86 years. Only high-quality scans revealing the entire sinus were included.

### Imaging protocol

All images were obtained using a NewTom 3G CBCT platform (Quantitative Radiology, Verona, Italy) with scan parameters: 94 kVp, 14 mA, and 27 s. In all three planes, images were examined (axial, sagittal, and coronal) by a single investigator (S.Y.) with the aid of Romexis dental software (Planmeca, Helsinki, Finland).

### Classification of the skeletal pattern and sphenoid sinus

The anteroposterior skeletal relationships of the maxilla and mandible were categorized as skeletal class I, II or III using the A point (the maxillary bone anterior limit)– nasion (nasofrontal suture anterior limit)– B point (the mandibular bone anterior limit) (ANB) angle [ANB angle 0–4° (class I), ANB angle >4° (class II), and ANB angle <0° (class III)] measured in the sagittal plane. First, the sagittal sections were evaluated and divided into conchal, presellar, and sellar (complete and incomplete) types according to the relationships with the anterior and posterior walls of the sellae turcica. In the conchal type, pneumatization extended for >10 mm beyond the anterior walls of the sellae turcica. In the presellar type, pneumatization did not advance above a vertical line commencing at the anterior pituitary fossa wall. In the sellar type, pneumatization extended over that line. In the incomplete sellar type, pneumatization continued beneath the anterior, but not the posterior, wall of the pituitary fossa; in the com-

plete sellar type, pneumatization proceeded past both walls (Figure 1). There are four types of pneumatization extension into the clivus: occipital, dorsal, subdorsal, and combined occipital-dorsal. In the subdorsal type, pneumatization did not extend below the vidian canal level or above the sellae's inferior margins. Pneumatization in the dorsal type extended above a line drawn from the sellae's floors to the dorsa sellae. Pneumatization in the occipital type extended below the horizontal plane level between the paired vidian canals' upper edges. The combined occipital–dorsal type indicates pneumatization extending from the dorsum top to below a horizontal plane along the vidian canals' the upper edges (Figure 2).

Next, the lateral sphenoid sinus extensions were evaluated on coronal sections. The sinuses were divided into two types, those with lateral and those with lesser wings. The lateral type was evaluated by reference to the vidian canal–foramen rotundum (VR) line. The lateral type, in which pneumatization extended beyond the VR line, comprised three subtypes: greater wing, pterygoid, and fully lateral. The greater wing pneumatization extended past the VR line; pterygoid pneumatization extended to the pterygoid process, and full lateral pneumatization involved both the greater wing and pterygoid process. Pneumatization of the lesser wing type extended toward the optic arrow and anterior clinoid process (Figure 3).

When sphenoid sinus pneumatization was evaluated on axial sections, the anterior sinus type exhibited an anterolateral

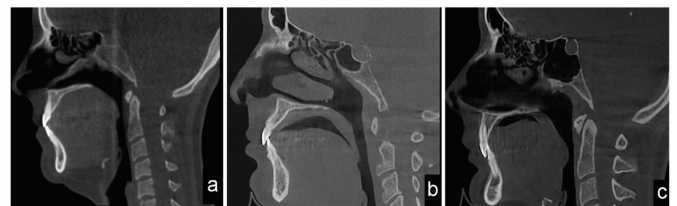


**Figure 1.** *a.* Presellar type, *b.* Incomplete Sellar type, *c.* Complete sellar type.

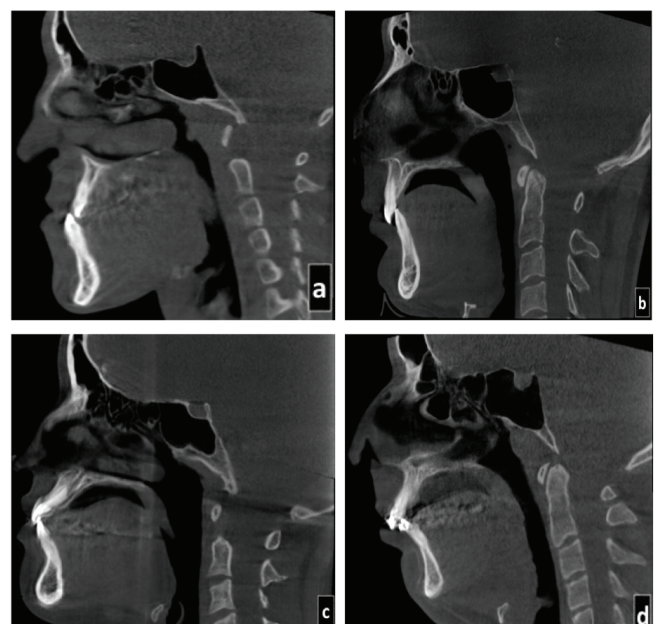


**Figure 2.** *a.* Dorsal type, *b.* Subdorsal type, *c.* Occipital type, *d.* Combined type..

protrusion extending past a transverse line drawn through the sphenoid crest at the sphenoid sinus side (Figure 4). All sphenoid sinuses were evaluated as described above.

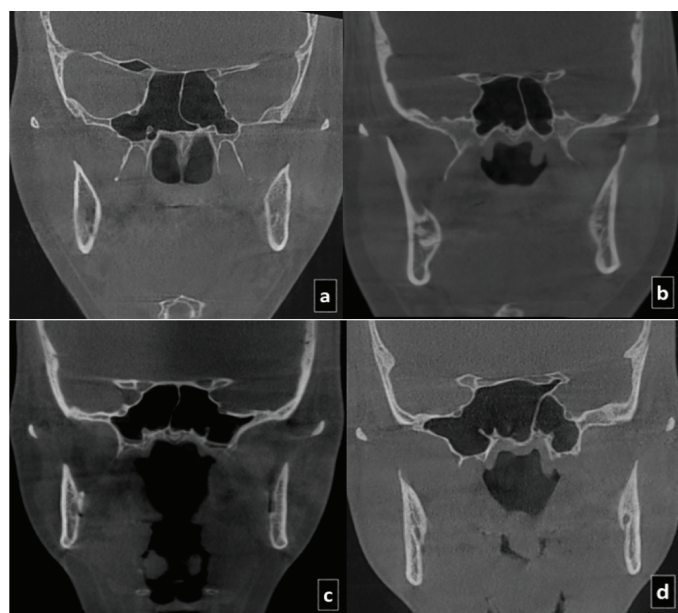


**Figure 3.** a. Right full lateral+lesser wing, left greater wing type, b. Bilateral pterygoid type, c. Bilateral full lateral type, d. Right full lateral, left pterygoid +lesser wing type.

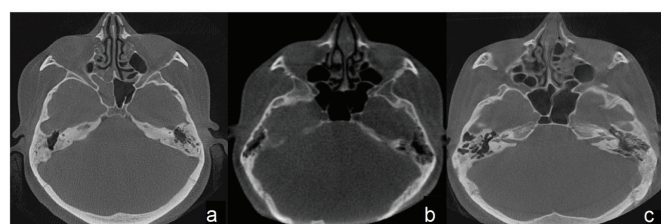


**Figure 4.** a, b. Bilateral anterior type, c. Left anterior type.

**Statistical analysis**

SPSS (version 20.0) software for Windows (IBM SPSS, Armonk, NY, USA) was used for all statistical analyses. The chi-squared test was used to assess between-group differences. P values less than 0.05 were considered statistically significant.

**Results**

We retrospectively analyzed CBCT images of 126 patients aged 18–86 years (mean 28.71 ± 13.11 years) in terms of sphenoid sinus pneumatization. The study population included 84 females (66.7%) and 42 males (33.3%), including 52 (41.3%) class I, 38 (30.1%) class II, and 36 (28.6%) class III cases. The conchal type of sphenoid sinus was not encountered. Presellar sinuses were detected in only 3 (5.8%) class I cases. Incomplete sinuses were detected in 16 (30.8%) class I, 7 (18.4%) class II, and 15 (41.7%) class III cases. Complete sinuses were detected in 33 (63.4%) class I, 31 (81.6%) class II, and 21 (58.3%) class III cases (Table 1); 67.4% exhibited clival extensions, most commonly the occipital type [23 (69.7%) class I, 21 (67.8%) class II, and 15 (71.4%) class III]. Lateral extensions were found in 103 (40.9%) of the 252 sinus walls:

33 (31.7%) in class I, 45 (59.2%) in class II, and 25 (34.7%) in class III sinuses. Full lateral extensions were most common, evident in 16 (48.5%) class I, 28 (62.2%) class II, and 17 (68%) class III cases (Table 2). The lesser wing type of pneumatization was in 22 (21.2%) class I, 27 (35.5%) class II, and 10 (13.9%) class III cases. Significant differences among the three sagittal skeletal groups were evident ( $p \leq 0.05$ ) in lesser wing pneumatization. Fifty sinuses (19.8%) were of the anterior type, most commonly in class I cases [24 (23.1%)] (Table 3). The distribution of the combined type sphenoid sinus based on the sagittal skeletal pattern is shown in Table 4.

**Table 1:** Distribution of pneumatization types based on the relation to anterior and posterior walls of sellae turcica by sagittal skeletal pattern.

| Pneumatization type | Sagittal Skeletal Pattern |                  |                  |            |
|---------------------|---------------------------|------------------|------------------|------------|
|                     | Class I                   | Class II         | Class III        |            |
| Conchal             | -                         | -                | -                |            |
| Presellar           | 3 (5.8%)                  | 0                | 0                |            |
| Sellar              | Incomplete sellar         | 16 (30.8%)       | 7 (18.4%)        | 15 (41.7%) |
|                     | Complete sellar           | 33 (63.4%)       | 31 (81.6%)       | 21 (58.3%) |
| <b>Total</b>        | <b>52 (100%)</b>          | <b>38 (100%)</b> | <b>36 (100%)</b> |            |

**Table 2:** Distribution of clival extension in 85 patients and distribution of lateral extension in 103 sinuses by sagittal skeletal pattern.

| Clival extension type  | Sagittal Skeletal Pattern |                  |                  |
|------------------------|---------------------------|------------------|------------------|
|                        | Class I                   | Class II         | Class III        |
| Subdorsal              | 6 (18.2%)                 | 5 (16.1%)        | 4 (19%)          |
| Dorsal                 | 2 (6.05%)                 | 0                | 1 (4.8%)         |
| Occipital              | 23 (69.7%)                | 21 (67.8%)       | 15 (71.4%)       |
| Combined               | 2 (6.05%)                 | 5 (16.1%)        | 1 (4.8%)         |
| <b>Total</b>           | <b>33 (100%)</b>          | <b>31 (100%)</b> | <b>21 (100%)</b> |
| Lateral extension type | Sagittal Skeletal Pattern |                  |                  |
|                        | Class I                   | Class II         | Class III        |
| Pterygoid              | 11 (33.3%)                | 12 (26.7%)       | 4 (16%)          |
| Greater wing           | 6 (18.2%)                 | 5 (11.1%)        | 4 (16%)          |
| Full lateral           | 16 (48.5%)                | 28 (62.2%)       | 17 (68%)         |
| <b>Total</b>           | <b>33 (100%)</b>          | <b>45 (100%)</b> | <b>25 (100%)</b> |

**Table 3:** Distribution of lesser wing and anterior type by sagittal skeletal pattern.

|                  | Sagittal Skeletal Pattern |                  |                  |
|------------------|---------------------------|------------------|------------------|
|                  | Class I                   | Class II         | Class III        |
| Lesser wing type | 22 (21.2%)                | 27 (35.5%)       | 10 (13.9%)       |
| Anterior type    | 24 (23.1%)                | 14 (18.4%)       | 12 (16.7%)       |
| <b>Total</b>     | <b>104 (100%)</b>         | <b>76 (100%)</b> | <b>72 (100%)</b> |

**Table 4:** Distribution of combined type by sagittal skeletal pattern.

| Combined type                       | Sagittal Skeletal Pattern |          |           |
|-------------------------------------|---------------------------|----------|-----------|
|                                     | Class I                   | Class II | Class III |
| Lesser wing+anterior                | 0                         | 1        | 0         |
| Lateral+anterior                    | 2                         | 0        | 2         |
| Lateral+lesser wing                 | 0                         | 0        | 1         |
| Clival+anterior                     | 4                         | 2        | 4         |
| Clival+lesser wing                  | 6                         | 4        | 2         |
| Clival+lesser wing+anterior         | 2                         | 3        | 0         |
| Clival+lateral                      | 10                        | 17       | 10        |
| Clival+lateral+anterior             | 8                         | 6        | 3         |
| Clival+lateral+lesser wing          | 9                         | 17       | 4         |
| Clival+lateral+lesser wing+anterior | 2                         | 1        | 0         |

## Discussion

The sphenoid sinus is the most changeable space in our body and is difficult to approach. Modern imaging techniques have improved our understanding of both normal and unusual anatomy, rendering surgery safer (10). Sellar access is markedly affected by sinus pneumatization, which ranges from absent to extensive; bone covering the carotid arteries and the optic and vidian nerves may be thin or even missing (11, 12). The first transsphenoidal surgery, initially performed in 1907, is now standard treatment for the sphenoid sinuses and intracranial lesions. Thus, the surgical anatomy of the sinus and adjacent regions must be understood (13). Sinus pneumatization has been explored by many authors. According to the extent of pneumatization around the sellae turcica, Hammer and Radberg (14) classified the sinus into sellar, presellar, and conchal types; this classification remains widely used. In recent years, transsphenoidal surgery has expanded to regions that bounded sphenoid sinus, such as the suprasellar region, middle cranial fossa, planum sphenoidale, clivus, cavernous sinus, and suprasellar region (15-20). Wang *et al.* (4) developed a new classification based on sinus extensions. They divided the sellar type of sphenoid sinus into six types including sphenoid body, lateral, clival, anterior, lesser wing, and combined type. Presellar sinuses were found in 2% of subjects; the conchal type was not encountered. The lowest prevalence observed from the sellar sinuses (98%) was lesser wing type, and the highest prevalence was combined type (59.2%). Hiremath *et al.* (21) classified the sphenoid sinus into conchal, presellar, and sellar (complete and incomplete) types based on the relationships of the sinus to the anterior and posterior walls of the sellae turcica, and classified clivus pneumatization as subdorsal, dorsal, occipital, or combined based on the relationships with the posterior wall, the sellae floors, and the vidian canal. The sellar (incomplete and complete), conchal and presellar types were found in 98.8% (22.2, and 76.6), 0, 1.2 of patients.

El-Kammash *et al.* (22) radiologically examined 182 cases; 3 (1.6%) evidenced conchal, 23 (12.6%) presellar, and 156 (85.7%) sellar pneumatization. On sagittal sections, we found that the sellar type was the most common (97.6%), in line with previous studies (1, 21-25). We did not encounter the conchal type, whose prevalence has been reported as 1–2% in previous studies of Caucasian and East Asian populations (4, 23, 24, 26, 27). We found presellar type sinuses in only 3 (5.8%) class I patients. Incomplete sinuses were detected in 16 (30.8%) class I, 7 (18.4%) class II, and 15 (41.7%) class III patients. Complete sinuses were detected in 33 (63.4%) class I, 31 (81.6%) class II, and 21 (58.3%) class III patients; these differences were not significant.

Wang *et al.* (4) classified posterior sinus pneumatization into dorsum, subdorsum, occipital, and dorsum–occipital types; the respective frequencies were 23.5, 63.2, 1.5, and 11.8%; the figures reported by Lu *et al.* (24) were 12.4, 71.9, 14.6, and 1.1%, and those by El-Kammash *et al.* (22) 7, 4, 3.5, and 5.7%. Hiremath *et al.* (21) reported that the subdorsal type was the most common (65%), followed by the dorsal (4%), combined (3.8%), and occipital types (3.8%). We found clival extensions in 65.7% of sinuses; the most common form was occipital [59 (46.8%) cases: 23 (69.7%) class I, 21 (67.8%) class II, and 15 (71.4%) class III] in contrast to previous studies. The differences were not significant.

Wang *et al.* (4) found lateral extensions in 92 (46%) of 200 sinus walls, including full lateral type in 71 (77%), the greater wing type in 11 (12%), and the pterygoid type in 10 (11%).

We found lateral extensions in 103 (40.9%) of 252 sinus walls: 33 (31.7%) in class I, 45 (59.2%) in class II, and 25 (34.7%) in class III cases. The full lateral extension was the most observed type in this study, as in that by Wang *et al.* (4). The prevalence of pneumatization of the greater wings or the pterygoid process ranged from 0 to 20% in the works of Idowu *et al.* (28), Hewaidi and Omami (29), and from 30 to 40% in the reports by Hewaidi and Omami (29), Sirikci *et al.* (30), and Kazkayasi *et al.* (31). El-Kammash *et al.* (22) found lateral extensions in 29.5% of all cases: greater wing type in 5.1%, full lateral type in 6.4%, and pterygoid type in 18%. Hiremath *et al.* (21) found the lesser wing type of pneumatization in 20.4% of all sinuses examined; the figure reported by El-Kammash *et al.* (22) was 7%. We detected the lesser wing type of pneumatization in 22 (21.2%) class I, 27 (35.5%) class II, and 10 (13.9%) class III cases; these frequencies differed significantly ( $p < 0.05$ ).

Most of the sphenoid sinus front wall is located behind the nasal turbinate, the ethmoidal air cells, and the sphenoid crest, the foremost part of the sinus. The anterior type of sinus features an anterolateral protrusion that advances above a transverse line drawn through the sphenoid crest on the side of the sinus (4). We found that 50 (19.8%) sinuses were of the anterior type, most commonly in class I cases (24; 23.1%). No significant among-group differences were evident. Wang *et al.* (4) found anterior type sinuses in 24 (12%) of 200 sides examined on 100 CT images. El-Kammash *et al.* (22) found such sinuses in 10 of 156 cases (6.4%) of sellar pneumatization.

## Conclusion

A highly pneumatized sphenoid sinus may disrupt the normal anatomical configuration. Anatomical sinus varia-

tions may render symptoms complex and cause potentially serious complications, such as injury to adjacent structures or cerebrospinal fluid leakage. Therefore, regional sphenoid sinus anatomy can be carefully examined via CBCT. We found that sphenoid sinus pneumatization did not differ significantly in patients exhibiting different types of sagittal skeletal closure, with the exception of the lesser wing type.

**Türkçe özet:** Farklı sagittal iskeletsel paternlerde sfenoid sinüsün konik ışınli bilgisayarlı tomografi ile değerlendirilmesi. Amaç: Bu çalışmanın amacı, çeşitli sagittal iskelet anomalileri olan bireylerde sfenoid sinüs varyasyonlarını konik ışınli bilgisayarlı tomografi (KİBT) kullanarak araştırmaktır. Gereç ve Yöntem: Yaşları 18-86 arasında değişen 126 hastanın KİBT görüntülerinde sfenoid sinüs pnömatizasyonunu geriye dönük olarak analiz ettik. Maksilla ve mandibulanın ön-arka iskelet ilişkileri, sagittal düzlemde ölçülen A noktası-nasion-B noktası (ANB) açısı kullanılarak iskeletsel sınıf I, II veya III olarak sınıflandırıldı. Sfenoid sinüsün uzantıları aksiyel, sagittal ve koronal olmak üzere üç düzlemde değerlendirildi. Bulgular: Çalışma popülasyonu 52 (%41,3) sınıf I, 38 (%30,1) sınıf II ve 36 (%28,6) sınıf III olmak üzere 84 kadın (%66,7) ve 42 erkek (%33,3) oluşturmuştur. Sfenoid sinüsün konikal tipine rastlanmadı. Sadece 3 (%5,8) sınıf I olguda presellar sinüs saptandı. 16 (%30,8) sınıf I, 7 (%18,4) sınıf II ve 15 (%41,7) sınıf III olguda eksik sinüs saptandı. 33 (%63,4) sınıf I, 31 (%81,6) sınıf II ve 21 (%58,3) sınıf III olguda tam sinüs saptandı. 252 sinüs duvarının 103'ünde (%40,9) lateral uzantı saptandı. Bunların oranı Sınıf I'de 33 (%31,7), sınıf II'de 45 (%59,2) ve sınıf III sinüslerde 25 (%34,7) olarak belirlendi. Sonuç: Bölgesel sfenoid sinüs anatomisi KİBT ile incelenebilir. Sfenoid sinüs pnömatizasyonu, küçük kanat tipi hariç, farklı tipte sagittal iskelet kapanması sergileyen hastalarda önemli ölçüde farklılık göstermedi. Anahtar kelimeler: sfenoid sinüs, konik ışınli bilgisayarlı tomografi, anatomi, anomaliler, maloklüzyonlar

**Ethics Committee Approval:** The Clinical Research Ethical Committee of Atatürk University approved the research protocol on 03/01/2019, number 2019/21 and the work adhered to all relevant principles of the Declaration of Helsinki and amendments and revisions thereof.

**Informed Consent:** Additional informed consent was obtained from all individual participants included in the study.

**Peer-review:** Externally peer-reviewed.

**Author contributions:** SY, ISB, ABY participated in designing the study. EK, ISB participated in generating the data for the study. EK participated in gathering the data for the study. EK participated in the analysis of the data. SY wrote the majority of the original draft of the paper. SY participated in writing the paper. SY has had access to all of the raw data of the study. SY has reviewed the pertinent raw data on which the results and conclusions of this study are based. SY, EK, ISB, ABY have approved the final version of this paper. SY, EK, ISB, ABY guarantee that all individuals who meet the Journal's authorship criteria are included as authors of this paper.

**Conflict of Interest:** The authors declared that they have no conflict of interest.

**Financial Disclosure:** The authors declared that they have received no financial support.

## References

1. Štoković N, Trkulja V, Dumić-Čule I et al. Sphenoid sinus types, dimensions and relationship with surrounding structures. *Ann Anat-Anatomischer Anzeiger*. 2016;203:69-76. [CrossRef]
2. Fujioka M, Young LW. The sphenoidal sinuses: radiographic patterns of normal development and abnormal findings in infants and children. *Radiology* 1978;129(1):133-6. [CrossRef]
3. Tan HK, Ong Y, Teo MS, Fook-Chong S. The development of sphenoid sinus in Asian children. *Int J Pediatr Otorhinolaryngol* 2003;67(12):1295-302. [CrossRef]
4. Wang J, Bidari S, Inoue K, Yang H, Rhoton Jr A. Extensions of the sphenoid sinus: a new classification. *Neurosurgery* 2010;66(4):797-816. [CrossRef]
5. Cheung D, Attia E, Kirkpatrick D, Marcarian B, Wright B. An anatomic and CT scan study of the lateral wall of the sphenoid sinus as related to the transnasal transthemoid endoscopic approach. *J Otolaryngol* 1993;22(2):63-8.
6. Mafee MF, Chow JM, Meyers R. Functional endoscopic sinus surgery: anatomy, CT screening, indications, and complications. *AJR Am J Roentgenol* 1993;160(4):735-44. [CrossRef]
7. DeLano MC, Fun F, Zinreich SJ. Relationship of the optic nerve to the posterior paranasal sinuses: a CT anatomic study. *Am J Neuroradiol* 1996;17:669-75. [CrossRef]
8. Yune HY, Holden RW, Smith JA. Normal variations and lesions of the sphenoid sinus. *Am J Roentgenol Radium Ther Nucl Med* 1975;124(1):129-38. [CrossRef]
9. Liu S, Wang Z, Zhou B, Yang B, Fan E, Li Y. Related structures of the lateral sphenoid wall anatomy studies in CT and MRI. *Lin chuang er bi yan hou ke za zhi= J Clin Otorhinolaryngol* 2002;16(8):407-9.
10. Simonetti G, Meloni F, Teatini G et al. Computed tomography of the ethmoid labyrinth and adjacent structures. *Ann Otol Rhinol Laryngol* 1987;96(3):239-50. [CrossRef]
11. Kinnman J. Surgical aspects of the anatomy of the sphenoidal sinuses and the sella turcica. *J Anat* 1977;124(Pt 3):541.
12. Hamid O, El Fiky L, Hassan O, Kotb A, El Fiky S. Anatomic variations of the sphenoid sinus and their impact on trans-sphenoid pituitary surgery. *Skull base* 2008;18(01):009-15. [CrossRef]
13. Perondi GE, Isolan GR, de Aguiar PHP, Stefani MA, Falcetta EF. Endoscopic anatomy of sellar region. *Pituitary* 2013;16(2):251-9. [CrossRef]
14. Hammer G, Rådberg C. The sphenoidal sinus: an anatomical and roentgenologic study with reference to transsphenoid hypophysectomy. *Acta Radiol* 1961(6):401-22. [CrossRef]
15. Cappabianca P, Cavallo LM, de Divitiis E. Endoscopic endonasal transsphenoidal surgery. *Neurosurgery* 2004;55(4):933-41. [CrossRef]
16. Cappabianca P, Cavallo L, Esposito F, De Divitiis O, Messina A, De Divitiis E. Extended endoscopic endonasal approach to the midline skull base: the evolving role of transsphenoidal surgery. *Adv Tech Stand Neurosurg Springer*; 2008. p. 151-99. [CrossRef]
17. Cavallo L, Cappabianca P, Messina A et al. The extended endoscopic endonasal approach to the clivus and craniovertebral junction: anatomical study. *Child's Nerv Syst* 2007;23(6):665-71. [CrossRef]
18. Cavallo LM, de Divitiis O, Aydin S et al. Extended endoscopic endonasal transsphenoidal approach to the suprasellar area: anatomic considerations—part 1. *Operative Neurosurgery* 2007;61(suppl\_3):ONS-24-ONS-34. [CrossRef]
19. de Divitiis E, Cavallo LM, Cappabianca P, Esposito F. Extended endoscopic endonasal transsphenoidal approach for the removal of suprasellar tumors: Part 2. *Neurosurgery* 2007;60(1):46-59. [CrossRef]
20. Kassam AB, Vescan AD, Carrau RL et al. Expanded endonasal approach: vidian canal as a landmark to the petrous internal carotid artery. *J Neurosurg* 2008;108(1):177-83. [CrossRef]
21. Hiremath SB, Gautam AA, Sheeja K, Benjamin G. Assessment of variations in sphenoid sinus pneumatization in Indian population: A multidetector computed tomography study. *Indian J Radiol Imaging* 2018;28(3):273. [CrossRef]
22. ELKammash TH, Enaba MM, Awadalla AM. Variability in sphenoid sinus pneumatization and its impact upon reduction of complications following sellar region surgeries. *Egypt J Radiol Nuclear Med* 2014;45(3):705-14. [CrossRef]
23. Anusha B, Baharudin A, Philip R, Harvinder S, Shaffie BM, Ramiza R. Anatomical variants of surgically important landmarks in the sphenoid sinus: a radiologic study in Southeast Asian patients. *Surg Radiol Anat* 2015;37(10):1183-90. [CrossRef]

24. Lu Y, Pan J, Qi S, Shi J, Zhang Xa, Wu K. Pneumatization of the sphenoid sinus in Chinese: the differences from Caucasian and its application in the extended transsphenoidal approach. *J Anat* 2011;219(2):132-42. [\[CrossRef\]](#)
25. Kajoak SA, Ayad CE, Balla EAA, Najmeldeen M, Yousif M, Musa A. Characterization of sphenoid sinuses for Sudanese population using computed tomography. *Glob J Health Sci* 2014;6(1):135. [\[CrossRef\]](#)
26. Sevinc O, Is M, Barut C, Erdogan A. Anatomic variations of sphenoid sinus pneumatization in a sample of Turkish population: MRI study. *Int J Morphol* 2014;32:1140-3. [\[CrossRef\]](#)
27. Vaezi A, Cardenas E, Pinheiro-Neto C et al. Classification of sphenoid sinus pneumatization: relevance for endoscopic skull base surgery. *Laryngoscope* 2015;125(3):577-81. [\[CrossRef\]](#)
28. Idowu O, Balogun B, Okoli C. Dimensions, septation, and pattern of pneumatization of the sphenoidal sinus. *Folia Morphol* 2009;68(4):228-32.
29. Hewaidi G, Omami G. Anatomic variation of sphenoid sinus and related structures in Libyan population: CT scan study. *Libyan J Med* 2008;3(3):1-9. [\[CrossRef\]](#)
30. Şirikci A, Bayazıt Y, Bayram M, Mumbuc S, Güngör K, Kanlıkama M. Variations of sphenoid and related structures. *Eur Radiol* 2000;10(5):844-8. [\[CrossRef\]](#)
31. Kazkayasi M, Karadeniz Y, Arikan OK. Anatomic variations of the sphenoid sinus on computed tomography. *Rhinology* 2005;43(2):109-14.